

Astronomical Notes

Astronomische Nachrichten

Rotating convection in f-boxes: Faster rotation

K. L. Chan

Department of Mathematics, The Hong Kong University of Science and Technology, Hong Kong

Received 2007 Aug 29, accepted 2007 Oct 10
Published online 2007 Dec 15

Key words convection – hydrodynamics – planets and satellites: general – stars: rotation – turbulence
Results based on 36 cases of f-box computations for different latitudes and rotation rates are summarized.

Astron. Nachr. / AN 328, No. 10, 1059–1064 (2007) / DOI 10.1002/asna.200710837

Rotating convection in f-boxes: Faster rotation

K. L. Chan*

Department of Mathematics, The Hong Kong University of Science and Technology, Hong Kong

Received 2007 Aug 29, accepted 2007 Oct 10

Published online 2007 Dec 15

Key words convection – hydrodynamics – planets and satellites: general – stars: rotation – turbulence

Results based on 36 cases of f-box computations for different latitudes and rotation rates are summarized.

© 2007 WILEY-VCH Verlag GmbH & Co. KGaA, Weinheim

1 Introduction

Numerical study of rotating convection usually takes one of the two approaches: global simulation of a spherical shell, *or* regional simulation of part of a shell. The first approach eliminates the introduction of artificial side boundaries, the second approach makes the resolution of small scales more affordable. For a discussion of the first approach, the readers are referred to the article by Meish in this volume. Here, we discuss some results of an investigation based on the second approach.

Regional simulation of rotating convection has a long history (e.g. Hathaway & Somerville 1983) and is still very popular (e.g. Brummel, Hurlburt & Toomre 2002). In astrophysics, these calculations take the rotation vector to be constant in the domain. We call it a ‘f-box’ configuration (a la ‘f-plane’ in geophysics).

2 Model

Our current calculations are similar to those described in Chan (2001); this includes the numerical scheme and the terminology. The basic differences are the resolution and the extended parametric range. For a $1.5 \times 1.5 \times 1$ box (width \times width \times height), $70 \times 70 \times 80$ grids are used. The stratification of the layer contains about 5 pressure scale heights. The lower 95% of the layer is convective, and the upper 5% is marginally stable. Using the box height, the initial density, pressure, and temperature at the top as units, the constant input flux at the bottom (F_{tot}) is 0.03125 (a lower boundary condition), and the fixed temperature at the top is 1 (an upper boundary condition). The box also has periodic side boundaries and stress-free upper and lower boundaries.

The computed cases provide a rather dense coverage of the latitude and the rotation rate. The colatitude (θ) has values $0, \pi/8, 2\pi/8, 3\pi/8, 7\pi/16, 4\pi/8$, and the rotation rate (Ω) has values $1/2^4, 1/2^3, 1/2^2, 1/2, 1, 3/2$. The rotation

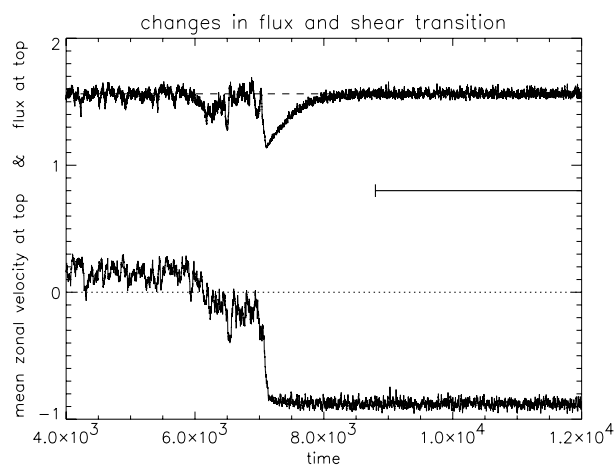


Fig. 1 An example of late stage transition ($\theta = \pi/2, \Omega = 0.6875$). The lower curve shows the mean zonal velocity at the top level of the region versus time. The upper curve shows the outgoing flux. The horizontal bar between the two curves on the right indicates a nominal length of time period used for computing statistical averages.

rates correspond roughly to Coriolis number ($Co \equiv \Omega \times$ total depth/root mean square turbulence velocity) values 0.37, 0.77, 1.7, 3.5, 7.5, and 12. An exception is the $\theta = \pi/2, \Omega = 3/2$ case in which supersonic flows occur. Including the reference case $\Omega = 0$, the total number of cases computed in this batch is 36. Cases with wider aspect ratios and more grid points have been computed, but some of them have not yet reached adequate thermal relaxation. We only discuss results based on the aspect ratio 1.5 cases here.

3 Relaxation

A stringent criterion has been adopted to judge the ‘relaxation’ of a calculation. The averaged outgoing energy flux (as well as the averaged total flux at any other level) has to be within 0.1% of the input energy flux from bottom. There are two reasons for this. First, we are interested in studying the relationship between the superadiabatic gradi-

* Corresponding author: maklchan@ust.hk

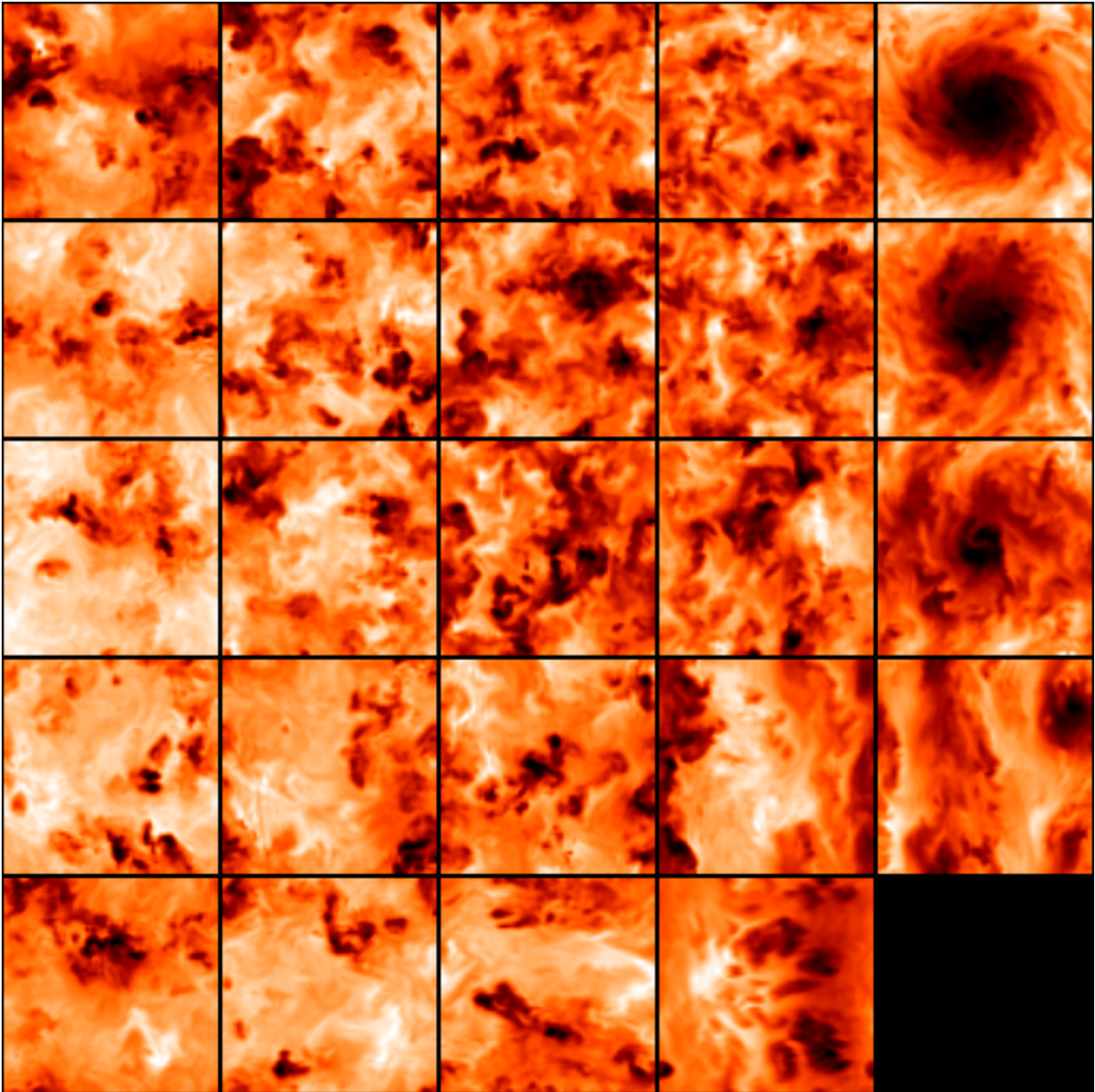


Fig. 2 (online colour at: www.an-journal.org) Horizontal cuts of temperature fields at the mid-level of the domain. The rows, from top to bottom, are for $\theta = 0, \pi/8, 2\pi/8, 3\pi/8,$ and $4\pi/8$; the columns, from left to right, are for $\Omega = 1/2^3, 1/2^2, 1/2, 1,$ and $3/2$. Light/dark shadings represent higher/lower temperatures.

ent and the rotation rate (modification to the mixing length theory). The superadiabatic gradient in the convection zone is a small quantity which depends delicately on the thermal structure. Second, this is an effort to avoid surprising flow transitions that may occur at a late stage of evolution toward relaxation. An example of such is shown in Fig. 1. The case is at the colatitude $\pi/2$ (equator) for the rotation rate $\Omega = 0.6875$. The Kelvin-Helmholtz time scale (τ_{KH}) is about 8000. The mean zonal velocity at the top of the region jump from positive to negative (corresponding to a reversal of vertical shear, see later discussion) at a rather late stage

of relaxation. The jump also produce a signature in the outgoing flux, with a time period lasting about one quarter of τ_{KH} .

4 A ‘mixing length’ relation

A preliminary fit to the numerical data yields the following approximate relationship between the local rms turbulence velocity v'' and the superadiabatic gradient ($\Delta\nabla$)

$$(v''/c_s)^2 \sim \Delta\nabla + R - f(\Omega)g(\theta), \quad (1)$$

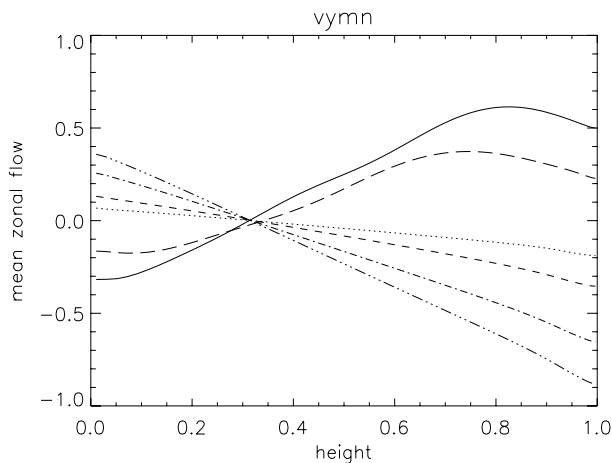


Fig. 3 Mean zonal velocity versus height. The dotted, dashed, dot-dashed, triple-dot-dashed, long-dashed, and solid curves are for the $\Omega = 1/2^3, 1/2^2, 1/2, 0.6875, 0.75, 1$ cases, respectively.

where $R = 0.0009$, $f(\Omega) = 0.0007\Omega\rho^{1/3}(1 + 0.1\Omega\rho^{1/3})$, $g(\theta) = 1 - 0.55\sin^6\theta$, and c_s is the local sound speed. The first three terms of this equation (one on the left and two on the right) describe the ‘mixing length’ relation in a non-rotating situation (Chan & Sofia 1989). The residual term R accounts for the existence of turbulence near the bottom of the convection zone where $\Delta\nabla$ crosses 0; understandably, it has a mild dependence on the strength of the total flux and the depth of stratification. The last term describes the inhibitive effect of rotation on the convective turbulence; the effect is maximized at the pole ($\theta = 0$). For the same v'' , a larger $\Delta\nabla$ is required to offset such effect.

5 Flow transitions

Figure 2 shows instantaneous horizontal cuts of temperature fields at the mid-level of the domain for cases at different latitudes (rows) and with different rotation rates (columns). Across the cases, several characteristics can be observed:

- Higher rotation generates smaller ‘granular’ cells.
- At and near the equator, as Ω increases, east-west oriented rolls are replaced by north-south oriented rolls.
- At and near the pole, as Ω reaches $3/2$, large dark spots appear. They correspond to large cyclonic vortices.

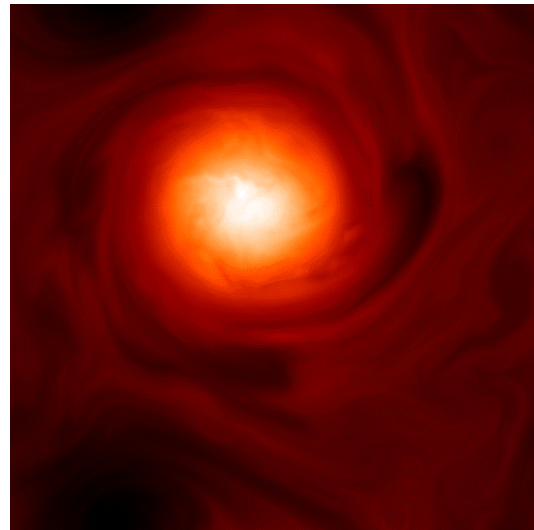


Fig. 4 (online colour at: www.an-journal.org) An anticyclone shows up as a hot spot.

The flow pattern transition at the equator (realignment of rolls) corresponds to a transition in the sign of the vertical shear of the mean zonal velocity (Käpylä, Korpi & Tuominen 2004). This is illustrated in Fig. 3 in which the vertical distributions of the mean (horizontally and temporally averaged) zonal velocity at the equator are shown. The profiles are very close to linear in the convection zone. The shear reverses sign between Ω values of 0.6875 and 0.75. For sufficiently large Ω , the mean zonal velocity increases outward (but with a small dip at the top).

We have computed different sets of cases with larger Coriolis numbers. Even anti-cyclonic vortices can be generated (Fig. 4). This may be relevant to planetary spots, but the discussion is to be postponed to another article.

Acknowledgements. This research is supported by the Hong Kong Research Grant Council (HKUST600306).

References

- Chan, K.L.: 2001, *ApJ* 336, 1022
 Chan, K.L., Sofia, S.: 1989, *ApJ* 336, 1022
 Brummell, N.H., Clune, T.L., Toomre, J.: 2002, *ApJ* 570, 825
 Hathaway, D.H., Somerville, R.C.J.: 1983, *JFM* 126, 75
 Käpylä, P.J., Korpi, M.J., Tuominen, I.: 2004, *A&A* 422, 793